

# Rule-Based Adaptive Control of an Isolated Intersection

SooJean Han<sup>1\*</sup>, Johanna Gustafson<sup>2</sup>, and Soon-Jo Chung<sup>1</sup>

**Abstract**—This project investigates the effectiveness of pattern-learning within a grid network of four-way intersections with Poisson arrivals. Here, patterns refer to intersection snapshots in the distribution of traffic, and we represent them using a vector of features such as the number of vehicles per lane and the average wait time. For a single intersection, we find that traffic congestion is substantially improved when using adaptive lights with camera sensors instead of the baseline periodic ones typically employed in the real-world today. We also investigate tradeoffs between several congestion metrics and the costs of installing sensor hardware such as cameras, which differ by pattern representation. We implement a framework for simulating traffic environments under simplifying traffic conditions such as Poisson arrival processes, then use real-world traffic data to show that the same insights hold with the simplifying assumptions removed.

## I. INTRODUCTION

In the problem of vehicle traffic congestion, periodic traffic lights often create suboptimal traffic flow, encouraging the necessity of adaptive signals and the additional sensing hardware needed to implement them. Moreover, adaptation to traffic flow is incorporated by installing cameras and sensors at intersections. While installing a large number of sensors may have higher efficiency in terms of control (e.g., whenever sensors sense vehicles in the vicinity, turn the corresponding light green), installing them may be very costly.

In our previous work [1], we showed that considering repeating patterns in the behavior of discrete stochastic systems allows for more efficient controller synthesis by eliminating computation time and redundancy in two ways: preserving past patterns into memory and predicting the future occurrence of patterns. In the context of traffic networks, repetition and structural symmetry arise naturally in a variety of ways. For example, many metropolitan intersection networks are typically arranged as a rectangular grid of parallel roads, where each intersection is 4-way, and the distance between adjacent intersections is near constant. For a single intersection, certain snapshots (e.g., a traffic camera photo which displays the number of vehicles present in each lane/direction of the intersection) often repeat over time, e.g., a snapshot containing  $X$  number of vehicles in the North-South lanes and no vehicles in the East-West lanes is likely

to occur again later in time; the converse snapshot where there no vehicles in the North-South lanes instead can be controlled analogously. Repetition can even be observed in the traffic density over time: for example, traffic may be heavy in the morning when people commute to work, light in the afternoon, heavy in the evening when people commute back, and light overnight. This behavior then repeats over the time of day for every day of the week (except potentially weekends).

These structural symmetries and repetitions over time suggest a control mechanism designed around some suitable choice of “pattern” representation has the potential for improving prediction accuracy and designing traffic lights to reduce congestion. As a result, we may also reduce monetary costs that come with sensor installation while still maintaining the congestion improvement achieved by pattern-learning and prediction.

## Related Work

Vehicle traffic control can be considered as a specific branch of problems in the broader topic of network congestion control. Hierarchical optimization and control for a related branch of problems in internet traffic congestion problems have been addressed in the past, see e.g., [2]. Models for solving vehicle traffic congestion problems have been proposed according to three primary levels of detail: microscopic, mesoscopic, or macroscopic [3]. At the microscopic level, one of the most common methods of modeling vehicle traffic is via queueing theory [4], [5], [6]. While appropriate to use as a benchmark for optimal performance, meaningful queueing theory results often rely on assumptions which are not reflective of real-world traffic (e.g., Poisson arrivals). Another subclass of microscopic models are discrete-time ODE dynamics [7], but these rely on the knowledge of parameters, e.g., the proportion of vehicles which turn right/turn left/go straight, whose values may be time-varying and would be difficult to obtain in practice. Moreover, many models are reliant on the assumption that there are enough sensors and cameras installed at every intersection so that an accurate portrayal of each intersection state can be captured.

Recently, data-driven architectures such as neural networks are gaining traction as suitable methods for congestion control due to their flexibility to more realistic traffic characteristics, adaptability to complex network topologies, and prediction capability. For example, [8] specifically leverages graph neural networks (GNNs) for computer network control and management. Towards vehicle congestion control, [9] developed a framework for automated incident detection based on Bayesian networks, with an emphasis on being

<sup>1</sup>SooJean Han and Soon-Jo Chung are with the Division of Engineering and Applied Science, California Institute of Technology, USA.

<sup>2</sup>Johanna Gustafson is with the Department of Engineering Physics, Lund University, Sweden.

\*Corresponding author. Email: soojean@caltech.edu

This paper is based on work supported by the National Science Foundation Graduate Research Fellowship under Grant No. DGE-1745301 and the Aerospace Corporation.

able to flexibly incorporate domain-specific knowledge from traffic experts into an otherwise all-data-driven approach. More recently, [10] considers a recurrent neural network (RNN) approach to characterizing the spatiotemporal behavior of vehicle traffic spread across complex network topologies. However, in the above-mentioned references for vehicle traffic application, the problem of developing efficient control strategies using these predictions and estimates is not addressed. Moreover, many of these neural network architectures are designed to account for general road network environments, and is wasteful when considering environments where topological symmetry may be leveraged, e.g., rectangular grids often found in metropolitan cities.

### Contributions

In this paper, we demonstrate that pattern learning and prediction have the potential to improve traffic congestion control in a single intersection by eliminating any unnecessary time and energy spent redundantly computing optimal light signal sequences in two ways. First, it preserves any intersection snapshots which have occurred in the past frequently enough to be deemed “interesting”; “interesting” patterns are stored into memory (e.g., in the form of a rule table) along with the corresponding light signal sequence which processes it. Second, it schedules future light signal sequences in advance by predicting future occurrences of the above-mentioned “interesting” intersection snapshots. In the vehicle congestion control context, the “patterns” that are represented correspond to the distribution of vehicles at each intersection (e.g., the number of vehicles per lane) in the network.

We then perform a comparison study of different rule-based adaptive traffic light signals over a variety of different congestion scenarios, similar to the study done in [11], in order to discern important tradeoffs in congestion improvement and sensor installation costs. First, because different pattern representations across different rule tables require different sensor hardware to gather the necessary data, we determine a suitable pattern representation for balancing the performance metrics with the sensor installation expenses. Second, we consider how the relative performances among the different rule tables vary under different traffic density scenarios. These tradeoffs determine the costs of being able to use the most of pattern learning and prediction to control the congestion in a single intersection.

## II. SETUP AND BACKGROUND

### A. Pattern-Learning Controller Framework

We begin by presenting the controller framework from [1], which differs from other standard controller implementations by the inclusion of *pattern learning and prediction*. Including a pattern-learning component enables a less redundant design of control input sequences for both the present and anticipated future based on an estimated observed.

**Definition 1 (Patterns).** Define the set  $\Psi \triangleq \{\psi_1, \dots, \psi_K\}$ , where each  $\psi_k \triangleq (\psi_{k,1}, \dots, \psi_{k,L})$  is a mode sequence with

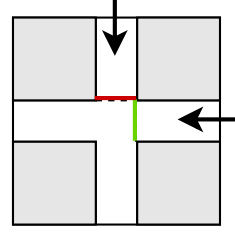


Fig. 1: A two-way intersection with incoming vehicles from E and N, with the green light given to E.

constant length  $L \in \mathbb{N}$  and elements  $\psi_{k,j} \in \mathcal{X}$ . Each  $\psi_k$  is referred to as a *(mode) pattern* if we are interested in observing its occurrence in the mode process  $\{\xi_n\}$  over time, e.g., because it models a system fault. We refer to  $\Psi$  as a *collection of patterns*. We use the notation of Definition 1 throughout the rest of the paper.

**Definition 2 (Pattern Occurrence Times).** Denote  $n \triangleq N[t] \in \mathbb{N}$  to be the current mode-index at current time  $t \in \mathbb{N}$ , and suppose the estimated current mode is  $\xi_n = \hat{\varphi}_n^{(t)}$ . Then for each of the patterns in the collection  $\Psi$  from Definition 1, define the following stopping times for each  $k \in \{1, \dots, K\}$ :

$$\hat{\tau}_{k|n}^{(t)} \triangleq \min\{i \in \mathbb{N} \mid \xi_n = \hat{\varphi}_n^{(t)}, \xi_{n+i-L+1:n+i} = \psi_k\} \quad (1)$$

**Definition 3 (Time and Probability of First Occurrence).** Under the setup of Definition 2 suppose  $\xi_{n+\hat{\tau}_n^{(t)}-L+1:n+\hat{\tau}_n^{(t)}} = \psi_k$ . Then define the following for the collection  $\Psi$ :

$$\hat{\tau}_n^{(t)} \triangleq \min_{k \in \{1, \dots, K\}} \hat{\tau}_{k|n}^{(t)}, \quad q_k^{(t)} \triangleq \mathbb{P}(\hat{\tau}_n^{(t)} = \hat{\tau}_{k|n}^{(t)}) \quad (2)$$

For the purposes of this application, we change the following parts of the setup from the original paper:

- mode process refers to intersection snapshots.
- No longer assuming the mode process has unknown distribution (we assume it’s Poisson). No longer assuming the modes are unobservable, although there is a sensor/hardware installation cost associated with every aspect of data we want to gather.
- No longer MJS and no longer Markov chain assumption. Could potentially leverage Poisson assumption, but might not be necessary because the mode process is observable. Also, the primary development in this paper is in the pattern-to-control sequence table, defined as  $\mathcal{U}$  in the original work.
- pattern learning is no longer based on a simple martingale scheme. Use a combination of (non-)homogeneous Poisson prediction and maximum likelihood. Don’t care about  $\mathbb{E}[\tau]$ .

### B. Single Intersection Model

Under a traffic signal control law which assigns the same light color to parallel directions, the standard four-way intersection over all directions E, N, W, S is a simple extension of a two-way intersection. Thus, for the sake of notation simplicity, we primarily consider the two-way intersection, with concrete directions chosen as E and N; a

sample visualization is shown in Figure 1. Each incoming and outgoing lane in the intersection has a fixed length, and the intersection itself has a fixed width. Vehicles enter into the intersection from direction  $\chi \in \{\mathbb{E}, \mathbb{N}\}$ . Each vehicle is identical with some length, and travels at a constant speed, which means it travels to and across the intersection at a fixed constant amount of time.

**Definition 4** (Intersection Quantities). We define the following quantities associated with the intersection and its lanes  $\chi \in \{\mathbb{E}, \mathbb{N}\}$ . The *arrival processes*  $\{N_\chi^{(a)}[t]\}_{t \in \mathbb{N}}$  of vehicles are such that  $N_\chi^{(a)}[t]$  defines the number of vehicles which have entered the intersection from lane  $\chi$  at time  $t$ , and abide by one of the distributions described in Section III-A. Moreover,  $\bar{N}_\chi^{(d)}[t]$  is defined to be the *total number of departed vehicles* along lane  $\chi$  which have left the intersection entirely by time  $t$ , and define the cumulative sum  $\bar{N}_\chi^{(d)}[t] \triangleq \sum_{\chi} \bar{N}_\chi^{(d)}[t]$ . Finally, define  $L_\chi[t] \in \mathbb{N}$  to be the *queue length* of vehicles in lane  $\chi$  at time  $t$ .

**Remark 1.** An arriving vehicle is only counted as a part of the queue length if one of the following two conditions holds. If the lane is empty, the vehicle joins the queue if it reaches the crossway. If the lane is not empty, the vehicle joins the queue if it reaches within minimum collision distance of the tail of the last vehicle currently in the queue.

**Definition 5** (Vehicle Quantities). Each vehicle  $i$  keeps track of the following quantities: 1) the direction  $\chi \in \{\mathbb{E}, \mathbb{N}\}$  from which it arrived, 2) its arrival time  $T_{\chi,i}$  to the intersection, and  $W_{\chi,i}[t]$  its cumulative wait time by time  $t$ , which increments by 1 timestep starting from the moment it stops at the red light and remaining constant when it passes and leaves the intersection on a green light.

**Definition 6** (Platoons). Each stream of traffic in the intersection is composed of (*vehicle*) *platoons*, determined based on their distance to each other; if two vehicles are within the minimum allowable collision-avoidance distance of each other, they are considered to be in the same platoon. The platoon membership of each vehicle can change over time, i.e., platoons may merge together as they move along the lane, and they can split apart by light signal interference.

**Definition 7** (Types of Sensors). We consider specifically two types of hardware: a camera sensor and vehicle to infrastructure (V2I) communication. For simplicity, we assume both types of sensors have the same *sensing region*  $\mathcal{B}_r$  for some fixed *sensing range*  $r \in \mathbb{R}^+$ : they are able to observe all vehicles in  $\mathcal{B}_r$ , which covers a maximum number of  $\bar{L} \in \mathbb{N}$  vehicles within a fixed distance  $r$  down each lane. When a *camera sensor* is installed at the intersection, it is able to count the number of vehicles in each platoon in  $\mathcal{B}_r$  and determine their positions away from the intersection stop line. When *V2I communication hardware* is installed at the intersection, it is able to collect the same information as a camera sensor and gauge the average waiting time of each platoon in  $\mathcal{B}_r$ .

**Definition 8** (Light Signal Quantities). The intersection is locally controlled by traffic lights, one per lane, and each take binary values depending on whether the light is green (1) or not (0). We define the value of the light signal along lane  $\chi$  to be  $u^{(\chi)}[t] \in \{0, 1\}$  at time  $t$ . Further define  $C_\chi[t]$  to be the *total number of complete (red-green) cycles* for lane  $\chi$  by time  $t$ , and define the interval of time  $[t_c, t_{c+1}) \subset [0, t]$  to be the *c-th cycle*, for  $c \in \{1, \dots, C_\chi[t]\}$  with *duration*  $D_{\chi,c} \triangleq t_c - t_{c-1}$  with  $t_0 \triangleq 0$ .

**Definition 9** (Congestion Metrics). Let  $[0, T]$  be the duration of simulation and define the following *congestion metrics* we use to evaluate the performance of each type of rule table on each type of arrival process: the *average cumulative waiting time* over all vehicles which have finished crossing the intersection by time  $T$  (see (3a)), the *average queue length per lane* in the intersection (see (3b)), the *average rate of intersection clearance* per lane  $\chi$  (see (3c)), the *proportion of vehicles that arrive on a green light* (see (3d)), and the *average number of light signal switches* (see (3e)).

$$W \triangleq \frac{1}{\bar{N}_\chi^{(d)}[T]} \sum_{\chi} \sum_{i=1}^{D_\chi^{(x)}} W_i[T] \quad (3a)$$

$$L \triangleq \frac{1}{2T} \sum_{\chi} \sum_{t=0}^T L_\chi[t] \quad (3b)$$

$$C_\chi \triangleq \frac{1}{C_\chi[T]} \sum_{c=1}^{C_\chi[T]} \frac{1}{D_{\chi,c}} (L_\chi[t_{c+1}] - L_\chi[t_c]) \quad (3c)$$

$$P \triangleq \frac{1}{2T} \sum_{\chi} \sum_{i=1}^{\bar{N}_\chi^{(d)}} \sum_{t=0}^T \mathbb{1}\{u^{(\chi)}[T_i^{(\chi)}] = 1\} \quad (3d)$$

$$S \triangleq \frac{1}{T-1} \sum_{t=0}^{T-1} \mathbb{1}\{u^{(\chi)}[t] \neq u^{(\chi)}[t+1]\} \quad (3e)$$

Here,  $N_\chi^{(a)}[t]$ ,  $\bar{N}_\chi^{(d)}[t]$ , and  $L_\chi[t]$  are from Definition 4;  $W_i[t]$  and  $T_i^{(\chi)}$  are from Definition 5;  $u^{(\chi)}[t]$ ,  $C_\chi[t]$ , and  $D_{\chi,c} \triangleq t_c - t_{c-1}$  are from Definition 8. The summation over  $\chi$ , wherever relevant, is done for  $\chi \in \{\mathbb{E}, \mathbb{N}\}$ , and in (3e),  $\chi$  is chosen to be any lane.

### III. INTERSECTION SCENARIO COMPARISONS

In this paper, our objective is to optimize over the sequence of light signals over time, which vary by traffic arrival process and adaptive rule table. We consider specifically the following different intersection scenarios.

#### A. Traffic Arrival Processes

The arrival processes  $\{N_\chi^{(a)}[t]\}_{t \in \mathbb{N}}$  of vehicles in each lane  $\chi \in \{\mathbb{E}, \mathbb{N}\}$  abide by one of the following distributions.

**Setting 1** (Homogeneous Standard Poisson). To each lane  $\chi \in \{\mathbb{E}, \mathbb{N}\}$ , vehicles arrive one-by-one according to some standard Poisson process with parameter  $\lambda_\chi$ . Each vehicle  $n \in \{1, 2, \dots\}$  has some associated arrival time  $T_n \in [0, T_{\text{sim}}]$ , with interarrival times  $S_n \triangleq T_n - T_{n-1}$  distributed exponentially, with  $T_0 \triangleq 0$ .

Pattern $[X_E, Y_N]$	Rule
$[L, 0], ([1, 0], \dots, [5, 0])$	Green to E until 0
$[L, L], ([1, 1], \dots, [5, 5])$	$[L, L] \rightarrow [0, L] \rightarrow [0, 0]$
$[L, L+1], ([1, 2], \dots, [4, 5])$	$[L, L+1] \rightarrow [L, 0] \rightarrow [0, 0]$
$[L, L+2], ([1, 3], \dots, [3, 5])$	$[L, L+2] \rightarrow [L, 0] \rightarrow [0, 0]$
$[L, L+3], ([1, 4], [2, 5])$	$[L, L+3] \rightarrow [L, 3] \rightarrow [0, 3] \rightarrow [0, 0]$
$[1, 5]$	$[1, 5] \rightarrow [0, 5] \rightarrow [0, 0]$

TABLE I: Sample rule table based only on considering number of vehicles per lane. The maximum number of vehicles in each lane which can be sensed by the camera is  $\bar{L}=5$ , so each table entry the appropriate  $L$ . For each given entry of the form  $[X, Y]$ , the case  $[Y, X]$  is controlled using the symmetric rule to  $[X, Y]$ .

**Setting 2** (Nonhomogeneous Standard Poisson). A nonhomogeneous arrival process is more reflective of real-world traffic characteristics than the previous homogeneous case. To each lane  $\chi \in \{E, N\}$ , vehicles arrive one-by-one according to some standard Poisson process with a time-varying parameter  $\lambda_\chi(t)$ . For example, this could reflect changes in traffic based on the time of day: between 10p and 6a,  $\lambda = 1$ , between 6a and 10a,  $\lambda = 5$ , between 10a and 12p,  $\lambda = 3$ , between 12p-1p  $\lambda = 5$ , etc. Moreover,  $\lambda_\chi(t)$  is often a periodic function, as vehicle arrivals tend to follow similar behavior every day of the week except possibly weekends.

**Setting 3** (Compound Poisson). Both of the above arrival processes can be extended to the case where multiple vehicles arrive simultaneously, as platoons. For each arrival time  $T_n$  of platoon  $n \in \{1, 2, \dots\}$ , the number of vehicles  $\xi[T_n]$  in the platoon is some random integer generated specifically from a multinomial distribution  $\mathcal{M} \triangleq \{1, \dots, M\}$  for a fixed maximum platoon size  $M \in \mathbb{N}$ . For each  $m \in \mathcal{M}$ ,  $\xi[T_n] = m$  with probability  $p_m \in [0, 1]$ .

#### B. Designing Adaptive Traffic Lights

We implement a menagerie of traffic light signals for congestion control in the single intersection described in Section II-B. The patterns from Definition 1 are interpreted to be the characteristics of the intersection snapshot and the vehicles within; we define what this means more concretely in the individual discussion of each adaptive signal.

**Setting 4** (Periodic Baseline). A single cycle of the intersection is given by one green phase of the E direction of traffic, followed by one red phase. Each cycle duration  $D_c$  is fixed at some period  $\Delta T$ , and the duration of the green phase is fixed at some constant proportion  $p\Delta t$  for some  $p \in (0, 1)$ .

**Setting 5** (Rule-Based Table: Number of Vehicles). The pattern representation from Definition 1 is a vector of the number of vehicles, arranged into a vector by lane  $\chi$ . A single camera sensor is used to collect the vehicle counts and queue lengths per lane. A rule-based table is constructed by assigning rules to every possible combination of vehicle

count profiles except the trivial case  $[0E, 0N]$ , which forms a total of  $(\bar{L} + 1)^2 - 1$  intersection snapshots. For computational efficiency, the entire combinatorial set of intersection snapshots are divided into multiple equivalence classes such that all snapshots in the same equivalence class are assigned the same rule (e.g.,  $[1E, 2N]$  is controlled the same way as  $[2E, 4N]$ ,  $[5E, 10N]$ , etc.). A sample rule table for  $\bar{L}=5$  is shown in Table I.

**Setting 6** (Rule-Based Table: Number of Vehicles and Average Platoon Waiting Time). The pattern representation from Definition 1 is the vector of the number of vehicles from Setting 5 and the vector of the average wait times of every platoon in  $\mathcal{B}_r$ . One V2I communication hardware is used to collect the above information per lane. The conditions of the table are constructed around the simple concept that platoons which have waited in the intersection for longer times should be allowed to pass more quickly. A more complex rule table based on this available data is shown in Figure 2. Here, the patterns are denoted by lists of 2-tuples of  $(N_i^{(x)}, W_i^{(x)})$  for all vehicles  $i$  which are within  $\mathcal{B}_r$ .

## IV. NUMERICAL SIMULATIONS

### A. Decision-making with Adaptive Lights

We consider an intersection for which that  $r = 50$  meters in  $\mathcal{B}_r$  and  $\bar{L} = 8$  vehicles for any sensor we use (see Definition 7). The arrival process of traffic is assumed to be stationary, homogeneous Poisson processes with  $\lambda_E 0.1$  vps and  $\lambda_N 0.2$  vps. We investigate the following three intersection scenarios. First, BP represents a baseline periodic light signal with a cycle period of 30s, 15s of which is spent green, with no sensor installations. Second, RTC represents the rule table from Setting 5 with a single camera sensor installation. Third, RTV represents the rule table from Setting 6 with V2I communication hardware.

Scenario	$W$	$L$	$C_N$	$P$	$S$
BP	4.981	1.828	0.000056	42.6%	10
RTC	3.369	1.272	-0.070765	60.8%	66.5
RTV	1.669	2.266	0.036034	57.4%	188

TABLE II: The congestion metrics of Definition 9 tabulated for three intersection scenarios, a baseline periodic signal, the rule-table adaptive signal from Setting 5, and the rule-table adaptive signal from Setting 6.

For 10 Monte-Carlo simulations over  $T = 300$ s simulation durations, the results are shown in Table II. The table shows that the adaptive traffic lights are shown to greatly reduce traffic congestion compared to a periodic baseline. The only metric wherein the baseline periodic traffic light is superior is the total number of green-to-red switches. We remark that the values in the average wait time and the number of switches suggest that an increasing frequency of traffic light switches allows for a reduction in the wait time. Another important

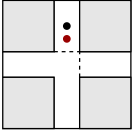
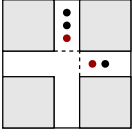
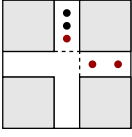
Intersection Snapshot	Traffic 1 ( $\chi_1$ )	Traffic 2 ( $\chi_2$ )	Rule
	Any number of platoons of vehicles in sensor range, e.g., $\{(N_i^{\chi_1}, W_i^{\chi_1})\}_{i=1}^k, k \in \mathbb{N}$	No vehicles / platoons: $\{\}$	Green to Traffic 1 until vehicle from Traffic 2.
	One platoon in sensor range, e.g., $\{(N_i^{\chi_1}, W_i^{\chi_1})\}$	One platoon in sensor range, e.g., $\{(N_i^{\chi_2}, W_i^{\chi_2})\}$	Green to Traffic 1 if $W_i^{\chi_2} + \frac{D_i^{\chi_2}}{v} \leq W_i^{\chi_1} + \frac{D_i^{\chi_1}}{v}$ else, Green to Traffic 2.
	Any number of platoons with length greater than 1, e.g., $\{(N_i^{\chi_1}, W_i^{\chi_1})\}_{i=1}^{k_1}, k_1 \geq 2$	Any number of platoons with length greater than 1, e.g., $\{(N_i^{\chi_2}, W_i^{\chi_2})\}_{i=1}^{k_2}, k_2 \geq 2$	Green to Traffic 1's first platoon if $\frac{1}{k_2} \sum_{i=1}^{k_2} \left( W_i^{\chi_2} + \frac{D_i^{\chi_2}}{v} \right) \leq \frac{1}{k_1} \sum_{i=1}^{k_1} \left( W_i^{\chi_1} + \frac{D_i^{\chi_1}}{v} \right)$ else, Green to Traffic 2's first platoon.

Fig. 2: Sample rule table based on considering both the number of vehicles per lane and the average waiting time. For each lane  $\chi$ , the total queue of vehicles is partitioned into some number  $k$  of platoons, and the rule is designed by considering the list of  $\{(N_i^{(\chi)}, W_i^{(\chi)})\}_k$ , where the  $N_i^{(\chi)}$  is the number of vehicles in platoon  $i$ , and  $W_i^{(\chi)}$  is the average waiting time of platoon  $i$ . In the leftmost column of the table, red dots represent vehicles which are the leading vehicle of their respective platoons. We define  $D_i^{\chi}$  to be the distance it takes for platoon  $i$  of lane  $\chi$  to fully cross the intersection, which is equivalent to the distance the last vehicle of the platoon must travel in order to fully cross the intersection.

trade-off to discuss is between the improvement of traffic congestion and the cost of installing sensor hardware. The difference between the congestion metrics of the adaptive traffic lights RTC and RTV is marginal, although RTV did consistently prove to be slightly better in its average rate of intersection clearance. But depending on the installation costs of each type of sensor, the difference may be negligible, and there would be little gain in using the more advanced and costly RTV.

### B. Varying Arrival Processes

Under the same intersection specifications and the BP and RTC scenarios described in Section IV-A, we now determine whether the tradeoffs observed for standard homogeneous Poisson arrivals also hold for the other arrival processes from Section III-A. The  $\lambda(t)$  used for nonhomogeneous Poisson arrivals is an artificially-constructed function with peaks placed at times where it is common to observe large amounts of traffic; see Figure 3 for an example. The multinomial distribution used for compound Poisson arrivals is  $[0.6, 0.2, 0.1, 0.05]$  for platoon sizes 1 to 4, respectively. For all 10 Monte-Carlo trials, the simulation time is increased to 12h (= 43200s) in order to mimic traffic between 8 am and 8 pm.

Results are presented in Tables III-VI. It appears that the adaptive traffic lights improve all congestion metrics across all queuing model variants, but to varying degrees. Similar to the results in Section IV-A, we find that  $B_1$  and  $C_1$  are superior to  $A_1$  in improving traffic congestion. Despite

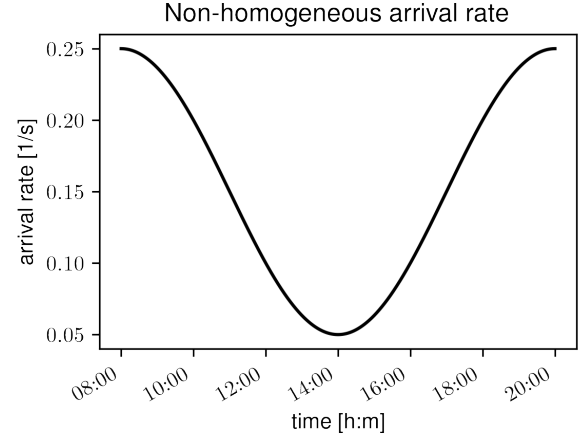


Fig. 3: The periodic arrival rate  $\lambda(t)$  for non-homogeneous Poisson arrival processes, modeled to exhibit peaks ( $\lambda(t) = 0.25$  vps) at 8 am and 8 pm, and a minimum at 2 pm ( $\lambda(t) = 0.05$  vps).

Scenario	$W$	$L$	$C_N$	$P$
BP <sub>1</sub>	4.187	0.477	0.000011	47.9%
RTC <sub>1</sub>	0.491	0.093	-0.007608	87.3%

TABLE III: Table II for standard homogeneous Poisson arrivals of different  $\lambda_\chi$  values (both are 0.1 vps).



Scenario	$W$	$L$	$C_N$	$P$
BP <sub>2</sub>	4.556	0.813	-0.000002	45.4%
RTC <sub>2</sub>	1.479	0.313	-0.024596	74.7%

TABLE IV: Table II for standard non-homogeneous Poisson arrivals with  $\lambda_\chi(t)$  as in Figure 3.

Scenario	$W$	$L$	$C_N$	$P$
BP <sub>3</sub>	4.556	0.813	0.000065	43.8%
RTC <sub>3</sub>	3.407	1.377	-0.027648	64.6%

TABLE V: Table II for compound non-homogeneous Poisson arrivals with  $\lambda_\chi(t)$  as in Figure 3.

using the same queuing model variant, the improvements in cumulative average waiting time and average queue length per lane are almost triple that of previous results (see Tables II versus III) and the difference in proportion arriving on green light is around twice as big, likely resulting from the differences in arrival rates. This increase in improvement can not be seen for the average rate of intersection clearance. With the addition of a varying arrival rate in the second variant (see Table IV), the improvement in traffic congestion through installing adaptive traffic lights is smaller although still significant.

The third variant with compound non-homogeneous Poisson arrivals has the heaviest traffic and also the smallest improvement for adaptive traffic lights. We can also see that there is a slightly better improvement in the average cumulative waiting time than in the average queue length per lane, relative what has been seen for the first and second variants. The last variant with compound homogeneous Poisson arrivals have results closer to that of the first variant, but similar to the previous variant, the improvement is lower for the average queue length per lane than the average cumulative waiting time.

Overall, we see that there is a correlation between the heaviness of traffic and the improvement in congestion through installing adaptive traffic lights, as opposed to periodic traffic lights. The variants 1-4 each have vehicle flow rates of around 0.10, 0.15, 0.20 and 0.13 vps respectively, which when placed in order of size (smallest to largest) corresponds to the order of improvement (largest to smallest), in relation to average cumulative waiting time and average queue length per lane. Figure 4 demonstrates this trend. It was also noted that in variants 3 and 4, with compound

Scenario	$W$	$L$	$C_N$	$P$
BP <sub>4</sub>	4.845	1.083	0.000005	46.2%
RTC <sub>4</sub>	0.945	0.337	-0.013168	80.6%

TABLE VI: Table II for compound homogeneous Poisson arrivals.

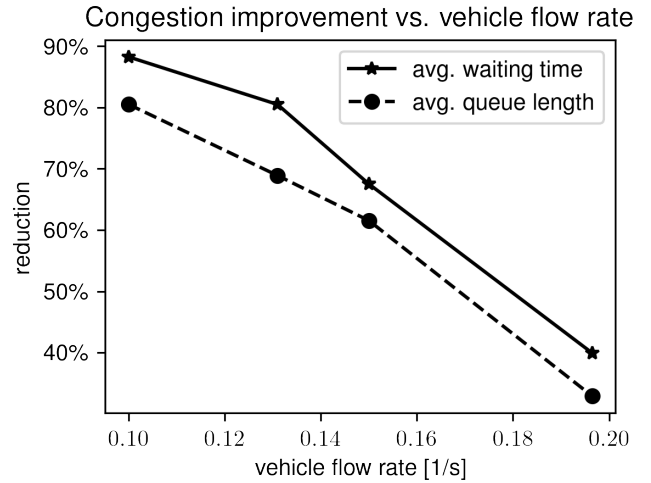


Fig. 4: The reduction in average cumulative waiting time and average queue length decreases as the vehicle flow rate per lane increases. Reduction values correspond to the difference between BP<sub>i</sub> and RTC<sub>i</sub> for  $i = 1 \dots 4$ .

Poisson arrivals, the improvements in average queue length per lane were slightly lower than in average cumulative waiting time, in relation to what was seen in variants 1 and 2. The reason for this is because platoons of vehicles arrive simultaneously as opposed to one by one with a few time-steps in between, meaning longer queues build up quicker within a lane and thus contributing to a slightly higher average.

### C. Extension to Real-World Traffic

To supplement the artificial arrival processes used in Sections IV-A and IV-B, we now evaluate the performance of each intersection configuration on a 3h long simulation by appending 3 of the provided 1h long real-world datasets collected from an intersection in Hangzhou, China [Link]. We remark that this dataset is for a standard four-way intersection, and the congestion metrics from Definition 9 are modified to average over each pair of non-conflicting directions where applicable (e.g., E,W are treated as one direction, while N,S are treated as the other). The arrival time of each vehicle is determined by the *startTime* parameter in the dataset. Any group of vehicles that arrive at the same time is considered a platoon, and counts as a single arrival. The datasets also detail the route of each vehicle, but for the purposes of this paper, we still assume straight-forward movement regardless of specified route. It's made apparent by figure 5 and table VII that the vehicles arrive in platoons with a varying average arrival rate, meaning the proposed queuing model with standard homogeneous Poisson arrivals wouldn't adequately represent this traffic environment. The average inter-arrival times and platoon size distributions are together equivalent to homogeneous arrival rates of 0.18 vps, 0.14 vps, 0.13 vps and 0.11 vps for each  $\chi \in \{N, E, S, W\}$ , respectively.

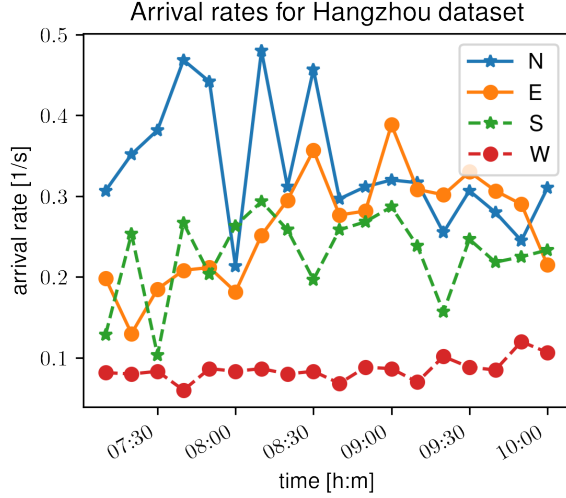


Fig. 5: Approximate arrival rates over time of each lane in the Hangzhou dataset (running average with 10-min window). Note that the x-axis only is accurate to scale.

$\chi$	avg.	st.d.	platoon size dist.
$N$	6.63 s	10.35 s	1: 78.5%, 2: 19.6%, 3: 1.5%, 4: 0.4%
$E$	8.49 s	12.12 s	1: 78.9%, 2: 19.5%, 3: 1.4%, 4: 0.2%
$S$	9.99 s	20.00 s	1: 75.2%, 2: 21.8%, 3: 2.2%, 4: 0.8%
$W$	11.68 s	17.84 s	1: 76.8%, 2: 22.4%, 3: 0.6%, 4: 0.1%

TABLE VII: Average and standard deviation of inter-arrival times and platoon size distributions in each lane of the Hangzhou dataset.

Scenario	$W$	$L$	$C_N$	$P$
BP	5.009	0.944	-0.000010	42.2 %
RTC	1.306	0.319	-0.019306	81.7 %
RTV	1.015	0.275	0.012590	77.5 %

TABLE VIII: Table II for the Hangzhou dataset.

- [9] K. Zhang and M. A. Taylor, “Effective arterial road incident detection: A Bayesian network based algorithm,” *Transportation Research Part C: Emerging Technologies*, vol. 14, no. 6, pp. 403–417, 2006.
- [10] Y. Li, R. Yu, C. Shahabi, and Y. Liu, “Diffusion Convolutional Recurrent Neural Network: Data-Driven Traffic Forecasting,” in *International Conference on Learning Representations*, 2018.
- [11] G.-L. Chang and C.-C. Su, “Predicting intersection queue with neural network models,” *Transportation Research Part C: Emerging Technologies*, vol. 3, no. 3, pp. 175–191, 1995.

## V. CONCLUSION

### REFERENCES

- [1] S. Han, S.-J. Chung, and J. C. Doyle, “Predictive control of linear discrete-time markovian jump systems via the analysis of recurrent patterns,” *Automatica*, Under review 2022.
- [2] M. Chiang, S. H. Low, A. R. Calderbank, and J. C. Doyle, “Layering as optimization decomposition: A mathematical theory of network architectures,” *Proceedings of the IEEE*, vol. 95, no. 1, pp. 255–312, 2007.
- [3] W. Burghout, H. Koutsopoulos, and I. Andreasson, “A discrete-event mesoscopic traffic simulation model for hybrid traffic simulation,” in *2006 IEEE Intelligent Transportation Systems Conference*, 2006, pp. 1102–1107.
- [4] A. J. Miller, “A queueing model for road traffic flow,” *Journal of the Royal Statistical Society: Series B*, vol. 23, no. 1, pp. 64–90, Jan 1961.
- [5] J. Lioris, R. Pedarsani, F. Y. Tascikaraoglu, and P. Varaiya, “Platoons of connected vehicles can double throughput in urban roads,” *Transportation Research Part C: Emerging Technologies*, vol. 77, pp. 292–305, 2017.
- [6] A. Muralidharan, R. Pedarsani, and P. Varaiya, “Analysis of fixed-time control,” *ArXiv preprint, arXiv:1408.4229*, 2015.
- [7] S. Coogan, E. A. Gol, M. Arcak, and C. Belta, “Controlling a network of signalized intersections from temporal logical specifications,” in *2015 American Control Conference (ACC)*, 2015, pp. 3919–3924.
- [8] K. Rusek, J. Suárez-Varela, P. Almasan, P. Barlet-Ros, and A. Cabellos-Aparicio, “Routenet: Leveraging graph neural networks for network modeling and optimization in sdn,” *IEEE Journal on Selected Areas in Communications*, vol. 38, no. 10, pp. 2260–2270, 2020.